Stepwise Reprogramming of B Cells into Macrophages

Huafeng Xie, Min Ye, Ru Feng, and Thomas Graf*
Department of Developmental and
  Molecular Biology
Albert Einstein College of Medicine
  Cancer Research Center
1300 Morris Park Avenue
Bronx, New York 10461

Summary

Starting with multipotent progenitors, hematopoietic lineages are specified by lineage-restricted transcription factors. The transcription factors that determine the decision between lymphoid and myeloid cell fates, and the underlying mechanisms, remain largely unknown. Here, we report that enforced expression of C/EBPα and C/EBPβ in differentiated B cells leads to their rapid and efficient reprogramming into macrophages. C/EBPs induce these changes by inhibiting the B cell commitment transcription factor Pax5, leading to the downregulation of its target CD19, and synergizing with endogenous PU.1, an ETS family factor, leading to the upregulation of its target Mac-1 and other myeloid markers. The two processes can be uncoupled, since, in PU.1-deficient pre-B cells, C/EBPs induce CD19 downregulation but not Mac-1 activation. Our observations indicate that C/EBPα and β remodel the transcription network of B cells into that of macrophages through a series of parallel and sequential changes that require endogenous PU.1.

Introduction

Blood cell formation is one of the classical systems in which to study mechanisms of vertebrate lineage determination. Hematopoietic lineages are specified in a stepwise process of binary decisions, starting with multipotent progenitors, which branch into a common lymphoid and a common myeloid progenitor that differentiate in turn into additional intermediate progenitors (Akashi et al., 2000a, 2000b). Each lineage exhibits a distinct gene expression pattern that is laid down and maintained by a set of more than a dozen lineage-restricted transcription factors that are part of a "transcription factor network" (Orkin, 2000; Sieweke and Graf, 1998). Since random combinations of several of these factors could, at least in principle, lead to far larger numbers of phenotypes than observed, there must be mechanisms that ensure a highly coordinated control of transcription factor network remodeling during commitment. This assumption is supported by enforced transcription factor expression experiments where, for example, ectopic expression of GATA-1 (a Zn finger protein) in transformed as well as normal myeloid precursor cells reprograms them into megakaryocytic/erythroid (MEP) cells, eosinophils, or mast cells, lineages

in which GATA-1 is normally expressed (Heyworth et al., 2002; Kulessa et al., 1995). Likewise, expression of GATA-1 in common lymphoid progenitors suppresses their lymphoid colony-forming capacity and induces their capacity to form MEP colonies (Iwasaki et al., 2003). These experiments also showed that altering the balance of lineage-restricted transcription factors can reverse commitment and that reprogramming involves not just activation of novel gene expression programs but also extinction of the original ones. At least in some cases, this involves direct transcription factor interactions such as those between GATA-1 and PU.1 (an ETS family factor) (Cantor and Orkin, 2001; Graf, 2002).

Which transcription factors determine the decision-making process between lymphoid and myeloid cell fates and how they do it remain largely unknown. Unlike in adult bone marrow, where lymphoid and myeloid compartments branch early, the fetal liver contains bipotent B cell/macrophage progenitors (B/M) (for review, see Katsura [2002]), suggesting that these two lineages are closely related. It has also been shown that certain onco-gene-immortalized B cell lines can be reprogrammed into macrophages by the *raf/ras* oncogenes (Klinken et al., 1988) and by an activated form of the M-CSF receptor (M-CSFR) (Borzillo et al., 1990). Although the cell conversion frequencies appeared to be low, in both studies, the resulting myelomonocytic cells had the same immunoglobulin rearrangements as the original B lineage cells. These changes must have therefore involved a complete shutdown of the B cell-specific gene expression program and its replacement by a macrophage-specific gene expression program. How does this happen?

B cell differentiation is initiated by the transcription factors E2A (a helix-loop-helix protein) and EBF, in whose absence B cells are arrested at a stage before DJ rearrangements. Together, these genes induce the transcription of many B cell-specific genes, including that of the B cell commitment factor Pax5. From the pro-B cell stage onward, Pax5 (a paired domain transcription factor) activates the expression of genes such as *CD19* and *blnk* while suppressing lineage-inappropriate genes such as *M-CSFR* (*c-fms*) and *Notch-1* (Kee and Murre, 2001; Schebesta et al., 2002). C/EBPβ (a bZip family transcription factor) may also play a role in B cell differentiation, since ablation of this factor, which is expressed predominantly in mature cells of the B lineage (Cooper et al., 1994), leads to a decreased number of B cells in the bone marrow (Chen et al., 1997). A transcription factor that is important for both B cell and macrophage formation is PU.1, since mice defective in this gene lack both lineages (reviewed in Schebesta et al. [2002]). This factor, which is expressed at lower levels in B cells than in macrophages (DeKoter and Singh, 2000), has been implicated in B/M lineage decisions, since low levels of PU.1 expressed in PU.1$^{-/+}$ fetal liver precursors promote B cell differentiation, while high levels promote macrophage differentiation (DeKoter and Singh, 2000). No transcription factors have yet been shown to be uniquely required for macrophage forma-

*Correspondence: graf@aecom.yu.edu

tion, although C/EBPβ$^{-/-}$ macrophages exhibit functional defects such as a decreased production of the inflammatory response cytokine IL-12 (Screpanti et al., 1995). In contrast, C/EBPα$^{-/-}$ mice lack granulocytes (Zhang et al., 1997), a defect that can be rescued if C/EBPβ is inserted into the C/EBPα locus (Jones et al., 2002). In short, B cell fate is determined by E2A, EBF, Pax5, and PU.1, while myelomonocytic cells (which include both macrophages and granulocytes) are determined by elevated levels of PU.1 as well as by C/EBPα and/or C/EBPβ.

Here, we show that enforced expression of C/EBPα and β in B cells leads to their rapid and efficient reprogramming into macrophages. This occurs through a complex process that is initiated by the coordinated inhibition of Pax5 activity, resulting in the downregulation of CD19, and the synergistic action between C/EBPα and PU.1, resulting in the activation of macrophage-specific genes.

Results

Enforced C/EBPα Expression Induces Mac-1 Expression in Primary B Cell Precursors

A retroviral approach was used to express myeloid transcription factors in primary B cell precursors. As shown in Figure 1A, the vectors encode either GFP or hCD4 alone ("control virus") or C/EBPα together with GFP/hCD4 ("C/EBPα virus"). To obtain B cell progenitors, CD19$^+$ cells were purified from the bone marrow of C57Bl/6J mice using magnetic bead selection, typically yielding >99% CD19$^+$ cells (Figure 1B). Control virus-infected cells, grown under conditions that support both B cell and myeloid cell development, remained CD19$^+$Mac-1$^-$ (Figure 1C). In contrast, cells infected with C/EBPα downregulated CD19 and upregulated Mac-1, with ∼60% of the cells becoming CD19$^-$Mac-1$^+$ after 4 days (Figure 1D). No changes were seen in the uninfected portion of the sample. The effect is also C/EBPα-specific, since cells infected with virus expressing the irrelevant FOG-1 transcription factor showed no changes (data not shown). The efficiency of the observed phenotypic conversion was dependent on the level of C/EBPα, since the proportion of "nonresponders" was 4% within the population of GFP high cells and 60% within that of GFP low cells (Figure 1E).

Tracing the Reprogrammed Cells to B Cells Using a Cre Lox Lineage Ancestry Approach

The formation of biphenotypic intermediates (Figure 1D) makes it unlikely that the resulting CD19$^-$Mac-1$^+$ cells arose by the selective outgrowth of contaminating myeloid precursors. However, we occasionally observed the appearance of macrophages in control virus-infected cultures kept for more than 1 week, a fact that could obscure the further analyses of the reprogrammed cells. To get around this problem, we crossed CD19 Cre knockin mice with R26R-EYFP conditional reporter mice, in which initiation of EYFP expression depends on Cre activity (Figure 2A). In this cross (in the following called "CD19 ancestry mice"), EYFP is expressed in ca. 90% and 50% of CD19$^+$ spleen and bone marrow cells, respectively, while essentially all Mac1$^+$ myelomonocytic cells are

EYFP$^-$ (Figures 2B and 2C). In bone marrow-derived CD19$^+$ cells from CD19 ancestry mice infected with C/EBPα/hCD4 virus, 65% of the hCD4$^+$ EYFP$^+$ cells downregulated CD19 and activated Mac-1 expression within 5 days (Figure 2D), while control virus-infected cells remained unchanged.

Mature B Cells from the Spleen Can Also Be Reprogrammed

To determine whether mature B cells can also be reprogrammed, we tested B cells from the spleen of CD19 ancestry mice. In these mice, ∼90% of the B cells are EYFP$^+$, while, of the EYFP$^+$ population, no cells were Mac-1$^+$ (Figure 2E). All EYFP$^+$ cells were found to also express the kappa chain, lambda chain, IgM, IgD, and/or IgG (Figure 2F). Next, we isolated CD19$^+$ spleen cells, infected them with C/EBPα, and seeded them on stroma supplemented with cytokines. As shown in Figure 2G, 31% of the cells became Mac-1$^+$ 3 days after infection. No phenotypic changes were seen in the control virus-infected EYFP$^+$ cells (data not shown). We conclude that immunoglobulin-expressing cells derived from the spleen can be reprogrammed although at lower efficiencies than B cell precursors from bone marrow.

Reprogramming of B Cell Precursors In Vivo

To determine whether a B to M conversion can also be observed in vivo, we isolated B220$^+$ B cell precursors from a bone marrow pool of CD19 ancestry mice, infected two aliquots with either C/EBPα/hCD4 virus or with control virus for 6 hr, and injected them into two sublethally irradiated RAG2$^{-/-}$γc$^{-/-}$ mice each. As shown in Figures 2H and 2I, for one animal analyzed 6 days after transplantation, 51% of the C/EBPα-expressing, EYFP$^+$ cells were CD19$^-$Mac-1$^+$ in the bone marrow and 32% in the spleen. No reprogrammed myeloid cells were observed in an animal transplanted with control virus-infected cells (Figure 2J). Similar results were obtained with the other pair of mice analyzed. The Mac-1$^+$ cells of the experimental mice were also Gr-1$^+$B220$^-$, and about 80% were L-selectin$^+$. Most of the reprogrammed cells also exhibited relatively low side scatter values, suggesting that the in vivo reprogrammed cells resemble monocytes but not granulocytes.

In Vitro Reprogrammed Cells Resemble Macrophages Based on Morphology and Phagocytic Capacity

Next, we characterized the in vitro reprogrammed B cells from CD19 ancestry mice in more detail. Six days after infection of CD19$^+$ bone marrow precursors with C/EBPα virus, 78% of the CD19$^-$Mac-1$^+$ cells also expressed Gr-1, a marker of granulocytes and a subset of monocytes, and 66% expressed F4/80, a marker of mature macrophages and myeloid dendritic cell precursors (Hume et al., 2002). The reprogrammed cells also exhibited dramatic morphological changes: while control virus-infected EYFP$^+$ splenic B cells were small and lacked granules (Figure 3A), C/EBPα-infected cells were large and contained granules (Figure 3B). Likewise, FACS analyses revealed that C/EBPα-infected EYFP$^+$ cells exhibited mean forward/side scatter values of 624 and 504, respectively, compared to 445 and 262 for the
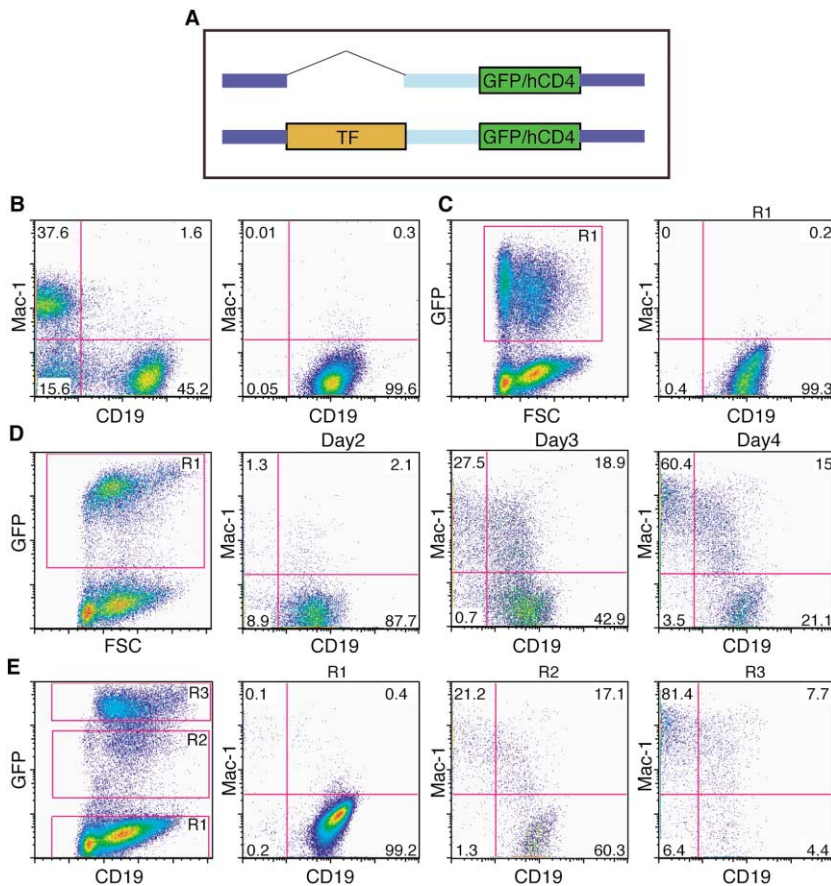
Figure 1. Induction of Mac-1 Expression in B Cell Precursors Infected with a C/EBPα Retrovirus

(A) Retroviral vectors used for infection (top, empty control vector; bottom, transcription factor [TF] encoding vector). Either GFP or hCD4 antigen was used as an indicator for infection. Dark blue boxes, retroviral LTRs; light blue boxes, IRES elements.
(B) FACS profiles of bone marrow cells before and after selection of CD19$^+$ cells, stained with Mac-1 and CD19 antibodies.
(C) Control virus-infected cells after 4 days culture, showing absence of CD19$^-$Mac-1$^+$ cells within the GFP$^+$ cell gate (R1).
(D) C/EBPα-infected cells showing increasing proportions of CD19$^-$Mac-1$^+$ cells as well as biphenotypic cells 2–4 days after infection.
(E) C/EBPα-infected cells (day 4) with gates corresponding to C/EBPα$^-$ (R1), low (R2), and high (R3) cells. Numbers in quadrants indicate percent marker-positive cells. FSC, forward scatter.

control virus-infected cells. When the S17 stromal cells plus remaining B cells were washed away, leaving strongly adherent macrophages behind, these were found to be phagocytic, including those that were EYFP$^+$ (inset in Figure 3B). As expected, control virus-infected cells were negative in this assay.

Gene Profiling Reveals Loss of Lymphoid Gene Expression and Upregulation of Macrophage-Specific Genes as well as PU.1

To study the gene expression pattern and functional properties of the reprogrammed cells, CD19$^+$ bone marrow cells from CD19 ancestry mice were infected with either control virus (Figure 3C) or C/EBPα/hCD4 virus (Figures 3D and 3E). Ten days later, cells in the indicated gates were sorted to yield control fractions 1–3. In addition, EYFP$^+$hCD4$^+$ cells (gate 4 in Figure 3D) were gated to reveal the fully reprogrammed CD19$^-$Mac-1$^+$ cells (Figure 3E). These were sorted for analysis (fraction 5). The RNAs of the four fractions were then analyzed by semiquantitative RT-PCR in comparison to RNAs from

CD19$^+$ and Mac-1$^+$ bone marrow cells (the latter contained both monocytes and granulocytes). As can be seen in Figures 3F–3H, while the three control fractions expressed all B cell markers tested, including the B cell transcription factor genes *EBF, Pax5, and E2A*, cells of fraction 5 showed no expression of the E2A/EBF target genes *RAG1, B29, Mb-1, λ5*, and *V-pre-B* nor that of the transcription factors *EBF, E2A*, and *Pax5* (there were trace amounts of *Mb-1* and *E2A* RNA). However, surprisingly, they still expressed significant levels of the *IL7-Rα* gene (a 2- to 3-fold reduction compared to B cell controls) not seen in the Mac-1$^+$ control fraction (Figure 3F). They also showed expression of all five monocytic markers tested, in particular *M-CSFR*, while the neutrophil markers scored negative except for one, *G-CSFR*, which was weakly expressed (Figures 3G and 3H). The reprogrammed macrophages in fraction 5 also differed from the B cell precursors in that they expressed 3- to 5-fold higher levels of PU.1 mRNA, reflecting similar differences as seen between the CD19$^+$ and Mac-1$^+$ controls from bone marrow (Figures 3G and 3I). We conclude that the in vitro reprogrammed cells resemble
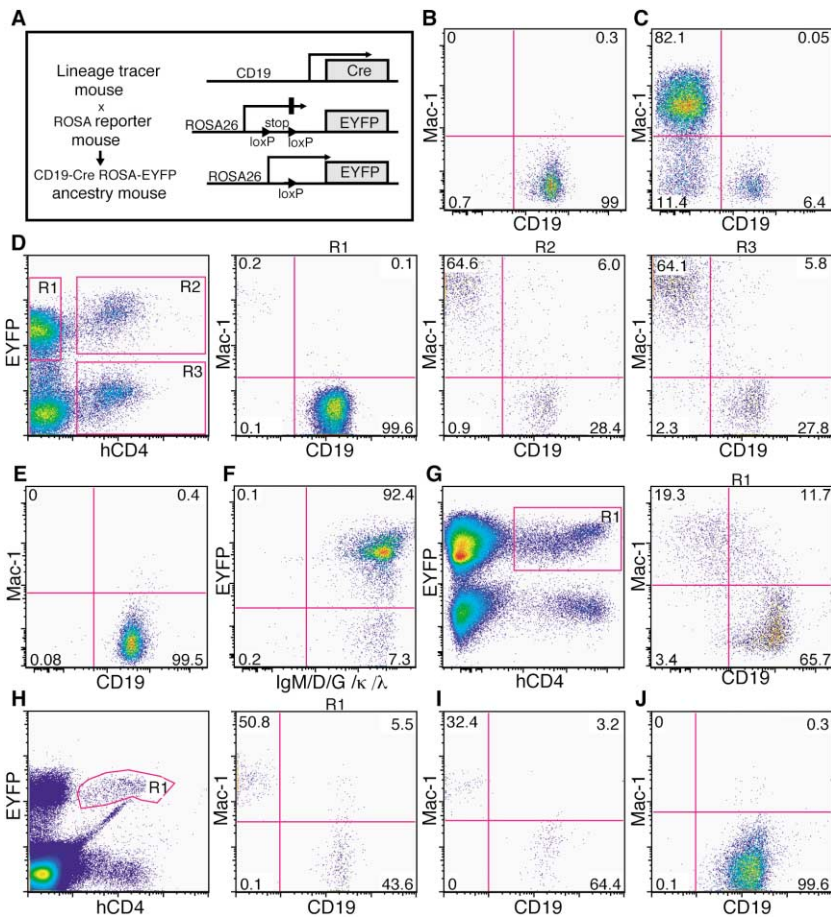
Figure 2. Cre Lox Lineage Ancestry Approach to Show Reprogramming of B Cells into Macrophages In Vitro and In Vivo

(A) Strategy outlining the generation of CD19 ancestry mice.

(B and C) Bone marrow cells from a CD19 ancestry mouse gated on the EYFP$^+$ population (B) and the EYFP$^-$ population (C) after staining with Mac-1 and CD19 antibodies.

(D) CD19$^+$ bone marrow cells from a lineage ancestry mouse infected with C/EBPα-hCD4 virus and cultured for 5 days, showing cells marked by CD19-Cre-mediated excision (EYFP$^+$-only cells, R1); EYFP-marked, infected cells (EYFP$^+$hCD4$^+$, R2), and unmarked, infected cells (hCD4$^+$ only, R3). Analysis of cells within these gates shows that, while the uninfected cells (R1) remain unchanged, the infected EYFP (marked R2) and unmarked B lineage cells (R3) reprogrammed with similar frequencies.

(E) Spleen cells from a CD19 ancestry mouse gated on the EYFP$^+$ population stained with Mac-1 and CD19.

(F) Purified CD19$^+$ spleen cells from CD19 lineage ancestry mice stained with IgM, IgD, IgG, kappa, and/or lambda chain antibodies.

(G) CD19$^+$ spleen cells from CD19 lineage ancestry mice infected with C/EBPα virus for 3 days, showing reprogramming frequencies of the infected, EYFP$^+$ cells (R1 gate).

(H) B220$^+$ bone marrow cells of CD19 lineage ancestry mice were infected with C/EBPα virus for 6 hr and transplanted into a sublethally irradiated immunodeficient mouse, and bone marrow was isolated 6 days later. The proportion of reprogrammed EYFP$^+$ cells is shown for cells present in gate R1 of one representative animal.

(I) Same as (H) but using the spleen for analysis.

(J) EYFP$^+$hCD4$^+$ spleen cells from a mouse transplanted with control virus-infected cells.

macrophages by morphological and functional criteria as well as by their gene expression profiles.

The Reprogrammed Macrophages Exhibit Both Heavy and Light Chain Immunoglobulin Rearrangements

During differentiation in the bone marrow, B cells undergo a series of heavy and light chain rearrangements. Cells with in-frame heavy chain VDJ rearrangements go on to rearrange their kappa or lambda light chains and display IgM on their surfaces. We therefore determined whether the reprogrammed macrophages derived from the B cell precursors of CD19 ancestry mice contain

immunoglobulin rearrangements. We detected both heavy chain DJ (Figure 3J) and VDJ rearrangements (Figure 3K and data not shown) in the reprogrammed macrophages but not in control bone marrow-derived macrophages. Selected bands were excised and a total of 35 clones sequenced, revealing 12 distinct VDJ rearrangements, of which four were in-frame. These included both proximal and distal V family members ([Chevillard et al., 2002], see Supplemental Table S1 at http://www.cell.com/cgi/content/117/5/663/DC1). The reprogrammed macrophages also exhibited kappa chain rearrangements not seen in the control macrophages (Figure 3L and data not shown). Three bands

were excised, and five distinct VJ rearrangements were observed among 27 kappa clones tested, two of which were in frame (Supplemental Table S2).

Downregulation of the Early B Cell Marker B220 Is Delayed

To gain more insights into the reprogramming process induced by C/EBPα, we monitored the C/EBP-induced cell surface antigen changes over time. The kinetics in Figure 4A shows that CD19 was downregulated more rapidly than was B220. Conversely, the proportion of Mac-1$^+$ cells increased more rapidly than Gr-1$^+$ cells, reaching a plateau at day 5. When plotting relative fluorescence intensities instead of percentage positive cells (Figure 4B), the differences between CD19 and B220 became even more significant, showing an ~70% reduction of CD19 expression at day 2, while B220 expression was slightly increased at this time point.

C/EBPβ Also Reprograms B Cells and Induces Cell Growth

Since C/EBPα is known to be functionally redundant with C/EBPβ within the hematopoietic system (Jones et al., 2002), we tested whether enforced expression of C/EBPβ can also induce the reprogramming of B cell precursors. The results in Figure 4C show that this is the case. Comparison of the two transcription factors in the same experiment revealed that the C/EBPα-induced Mac-1 upregulation was slightly faster, while the downregulation of CD19 was very similar for both factors (Figure 4D). The majority of the cells reprogrammed by C/EBPβ, as with C/EBPα, expressed Gr-1 and F4/80 antigens (data not shown). Remarkably, while the percentage of C/EBPα-infected cells decreased over time, the percentage of C/EBPβ-infected cells increased significantly in comparison to uninfected and control virus-infected cells (Figure 4E).

Exogenous PU.1 Collaborates with C/EBPα in B Cell Reprogramming

Since C/EBP and PU.1 are known to coregulate many macrophage-specific genes, a plausible explanation for the rapid C/EBP-induced reprogramming is that it does so by synergizing with endogenous PU.1. Based on this assumption, the C/EBP nonresponders might represent cells that express subthreshold levels of PU.1 and thus should be reprogrammable when coinfected with both C/EBPα and PU.1 viruses. To test this, CD19$^+$ bone marrow cells were coinfected with C/EBPα/hCD4 and PU.1/GFP virus. The cells were then analyzed by FACS at various times after infection and single- and double-infected as well as uninfected cell populations gated. As can be seen in Figure 5, the proportion of reprogrammed (CD19$^-$Mac-1$^+$) cells increased from 57% in C/EBPα only (R1) to 92% in the double-infected population (R2). More strikingly, the proportion of nonresponders decreased from 32% to 1.5% in the double-infected population. This effect is probably not due to the selective death of the nonresponders by high PU.1 expression, since similar survival rates were observed with single- and double-infected cells (data not shown). Unexpectedly, ~9% of the PU.1-only-infected cells (R3) also became CD19$^-$Mac-1$^+$, while no such cells were seen in

the uninfected cell population. As shown in Figure 5B, this result could be confirmed when CD19$^+$ cells were infected with PU.1 virus only. The results in this figure also indicate that, unlike C/EBP, enforced expression of PU.1 does not lead to the rapid downregulation of CD19. Finally, the data in Figures 5C and 5D show that coinfection of C/EBPα with PU.1 accelerates the formation of Mac-1-expressing cells without modifying the kinetics of CD19 downregulation. In conclusion, these data show that PU.1 synergizes with C/EBPα in reprogramming "nonresponders" and that the two factors cooperate in the activation of Mac-1 expression.

Mac-1 Activation but Not CD19 Downregulation Requires Endogenous PU.1

To test whether the induced B to M conversion requires endogenous PU.1, we expressed C/EBPα in a PU.1-defective pre-B cell line recently developed in our laboratory. This fetal liver-derived cell line expresses CD19 as well as most B cell-specific genes tested, including Pax5 and low levels of IL-7R but not B220, and also exhibits DJ and VDJ rearrangements (M.Y. and T.G., unpublished data). The cells were infected with either C/EBPα or PU.1 virus alone or with a combination of both and then analyzed 2–4 days later by gating on the infected cells. As a control, cells were infected with the corresponding control virus. As can be seen in Figure 5E, CD19 expression was downregulated by C/EBPα alone and by C/EBPα plus PU.1 at similar efficiencies but not by PU.1. Conversely, while neither PU.1 alone nor C/EBPα led to an upregulation of Mac-1 expression, 68% of the double-infected cells expressed the antigen after 4 days (Figure 5F). Finally, while PU.1 alone did not up regulate Gr-1 expression, 23% of the cells infected with C/EBPα expressed the antigen at day 4 compared to 83% of cells infected with C/EBPα plus PU.1 (Figure 5G). The control virus showed no effect, while very similar results as with C/EBPα were obtained when C/EBPβ virus was used for double-infection experiments (data not shown). These data show that induction of Mac-1 (and to a lesser extent Gr-1) expression by C/EBP requires endogenous PU.1, while its capacity to induce CD19 downregulation does not. They also confirm our observation that high levels of PU.1 do not inhibit CD19 expression.

Expression of Endogenous Mac-1 Is Activated in Fibroblasts by a Combination of C/EBP and PU.1

The above experiments raised the possibility that C/EBPα, together with PU.1, directly activates expression of the *Mac-1* gene. However, while the Mac-1 promoter has been described to contain PU.1 binding sites and to be PU.1 responsive, it was not reported to contain C/EBP binding sites (Pahl et al., 1993). Since, in these studies, only a 93 bp upstream fragment was tested, it seemed possible that C/EBP-responsive sites are present elsewhere in the Mac-1 promoter/enhancer. To test this, we infected NIH3T3 fibroblasts with a combination of C/EBPα and PU.1 and analyzed the cells by FACS 4 days later, gating on double- as well as single-infected cells. As shown in Figure 5H, the combination of C/EBPα and PU.1 strongly activated Mac-1 expression (about
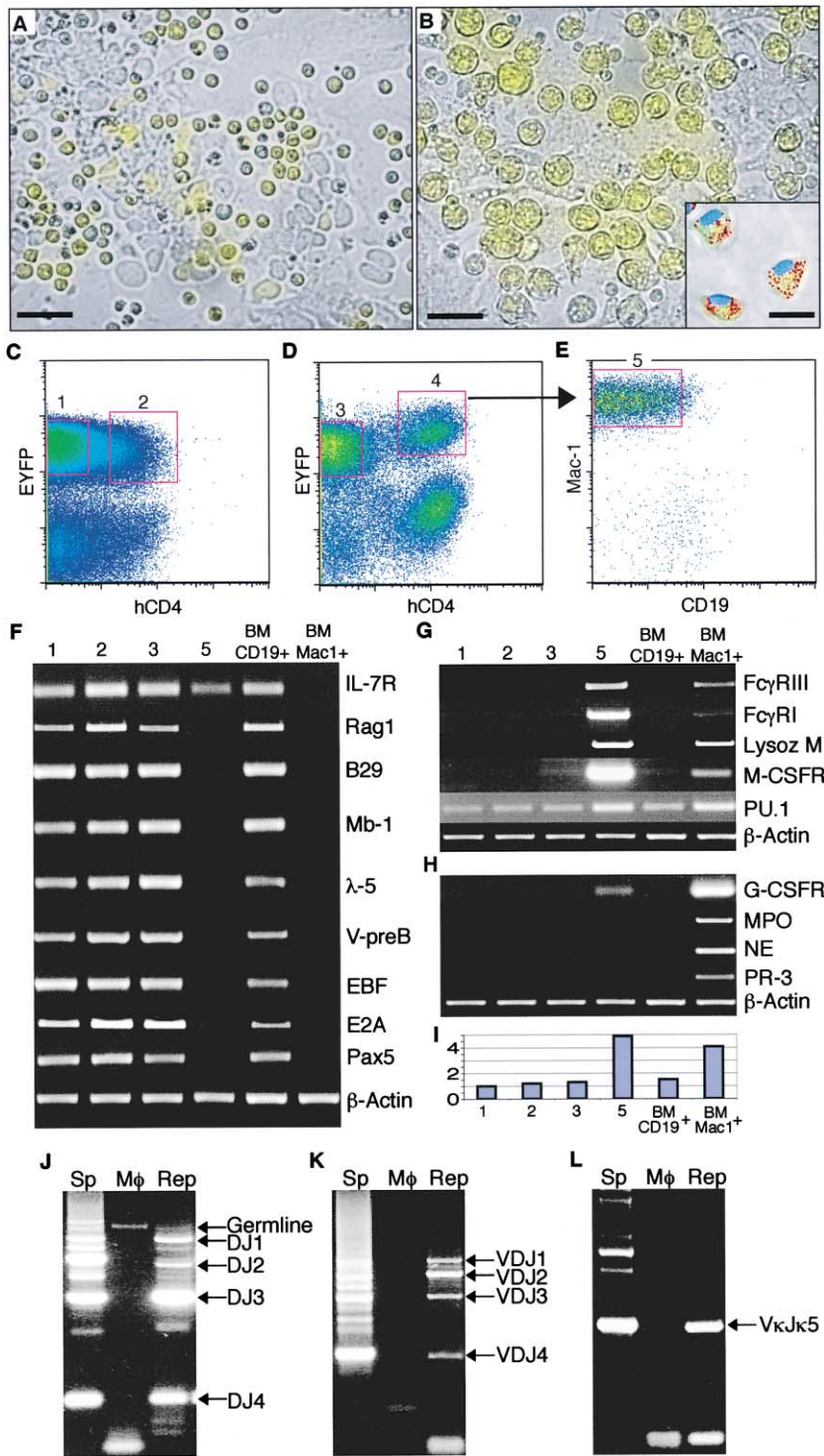
Figure 3. Phenotype of Reprogrammed Cells

(A and B) Morphology of CD19$^+$ spleen cells from CD19 ancestry mice infected and cultured for 10 days with either control virus or C/EBPα virus, respectively, showing EYFP$^+$ cells in yellow. The inset shows cells that have ingested red fluorescent beads, with nuclei stained blue with Hoechst 33342. Bars represent 20 μm.

(C–E) Cells used for RT-PCR analysis. CD19$^+$ bone marrow cells from CD19 ancestry mice were infected with control (C) or C/EBPα virus (D), cultured for 10 days, and analyzed by FACS, following staining with CD19 and Mac-1 antibodies. Cells in gates 1, 2, and 3 were sorted and served as negative controls. In addition, EYFP$^+$hCD4$^+$ cells in gate 4 (D) were plotted to reveal EYFP$^+$CD19$^-$Mac-1$^+$ cells (E) that were sorted for analysis (fraction 5).

(F–H) RT-PCR analysis of fractions 1, 2, 3, and 5, using the primers that detect the indicated genes ([F], B-lymphoid; [G], macrophage; [H],

60% of the cells showed a 30-fold increase in fluorescence intensity compared to uninfected control cells), while PU.1 alone weakly induced Mac-1 expression, and C/EBPα had essentially no effect (Figures 5I and 5J). Although we have not delineated the C/EBP-responsive element in the regulatory region of the *Mac-1* gene, our data are consistent with the notion that the gene is activated by the concerted action of PU.1 and C/EBP.

C/EBPα but Not PU.1 Inhibits the Capacity of Pax5 to Activate the CD19 Promoter

The rapid downregulation of CD19, a direct target of Pax5 (Kozmik et al., 1992; Schebesta et al., 2002), raised the possibility that C/EBP antagonizes Pax5 activity. We therefore transfected a CD19 promoter luciferase reporter construct containing a 1.3 kb upstream fragment of the human CD19 gene into 293 cells (a kidney-derived human fibrablastoid cell line) together with different concentrations of Pax5 DNA. As shown in Figure 6A, the luciferase activity increased gradually, reaching an approximately 2.5-fold increase at 0.05 μg of Pax5 DNA. Although this increase was modest, it was highly reproducible. No activation of the reporter was seen with C/EBPα, PU.1, or FOG-1 DNA (Figures 6B and 6C and data not shown). When the cells were cotransfected with 0.05 μg Pax5 DNA plus increasing amounts of a plasmid encoding C/EBPα, PU.1, or FOG-1, the luciferase reporter was inhibited by C/EBPα but not by PU.1 or FOG-1 (Figures 6D–6F). C/EBPβ, like C/EBPα, was also found to inhibit Pax5 activity (data not shown). Since the same expression vectors were used for both Pax5 and C/EBP, it is unlikely that the effects observed resulted from the inhibition of Pax5 expression. In conclusion, our results suggest that C/EBPα (and C/EBPβ) specifically inhibit Pax5 activity on the CD19 promoter.

Discussion

Our results show that B cells can be rapidly and efficiently reprogrammed to become macrophages after enforced expression of C/EBPα or C/EBPβ transcription factors. We were able to follow cell surface marker changes in large cell populations over time (Figure 7A) and to correlate them to modulations in the activity of key transcription factors acting on the promoters of relevant lineage marker genes (Figure 7B). C/EBP initiates the reprogramming process by simultaneously downregulating late lymphoid marker(s) and upregulating myeloid markers. Subsequently, one or more reprogramming waves lead to the complete extinction of early lymphoid markers and the generation of functional macrophages.

Can Mature B Cells Be Reprogrammed by C/EBP?

Our data indicate that at least 30% of the infectable immunoglobulin-expressing splenic B cells can be reprogrammed by enforced C/EBPα expression. We do not think that this observation can be explained by the selective outgrowth of a contaminating non-B lineage population since (1) the purified CD19^{+} cells used for infection, obtained from the CD19 ancestry mouse (which do not exhibit EYFP expression in *any* myeloid cells), were 99.2% pure and contained <0.1% Mac-1^{+} cells; (2) two days after C/EBPα infection, ~15% of the cells became Mac-1^{+}, while ~10% expressed intermediate levels of both CD19 and Mac-1 (data not shown); and (3) we did not detect significant differences in the cell cycle status between the reprogrammed and the nonreprogrammed cells in the C/EBP-infected samples 3 days after infection (not shown). Our data also suggest that every single CD19^{−}/Mac-1^{+} cell that was seen after C/EBPα expression (Figure 2G) is derived from an immunoglobulin-expressing cell, since essentially all of the EYFP^{+} cells in these mice express IgM, IgD, or IgG. Finally, the reprogrammed B cells correspond to functional macrophages, as illustrated in Figures 2A and 2B. The plasticity of B cells is surprising, since common lymphoid progenitors as well as pro-T (pro-T1) cells can be converted into myeloid cells after ectopic expression of human IL-2 or GM-CSF receptor, while this was no longer possible with either pre-T (pro-T2) cells or pro-B and pre-B cells (Iwasaki-Arai et al., 2003; King et al., 2002; Kondo et al., 2000).

What Myeloid Cell Types Are Generated?

That the in vitro reprogrammed B cells resemble macrophages was surprising, since C/EBPα is believed to play a role in the formation of granulocytes but not of macrophages. Thus, enforced C/EBPα expression in HL60 cells converts them into neutrophil granulocytes (Radomska et al., 1998), and C/EBPα transforms E26-MEP cells into eosinophil granulocytes. In contrast, both PU.1 and C/EBPβ convert E26-MEP cells into macrophage precursors (Nerlov and Graf, 1998; Nerlov et al., 1998). We cannot rule out the possibility that the lack of granulocytes observed in the present work is a result of the culture conditions used, although macrophages were also obtained when GM-CSF and G-CSF were added to the S17 stromal cultures (which produce M-CSF). The phenotype of both C/EBPα- and C/EBPβ-reprogrammed cells (Mac-1, F4/80, Gr-1, and L-selectin[+]) is characteristic of inflammatory-type monocytes (Geissmann et al., 2003), perhaps reflecting the fact that C/EBPβ becomes activated in monocytes during inflammatory responses (Poli, 1998).

---

neutrophil restricted genes). BM CD19^{+} and BM Mac-1^{+} are control fractions isolated from fresh bone marrow, containing B lineage cells and granulocytes/macrophages, respectively.
(I) Relative expression levels of PU.1, as determined by densitometry of samples analyzed by semiquantitative RT-PCR relative to β actin used as internal control.
(J–L) Immunoglobulin rearrangements of EYFP^{+}CD19^{−}Mac-1^{+} reprogrammed cells. The first lane (Sp) shows DNA from spleen cells, the middle lane (Mφ) corresponds to DNA from bone marrow-derived macrophages, and the last lane (Rep) corresponds to EYFP^{+}CD19^{−}Mac-1^{+} reprogrammed cells. (J), heavy chain DJ rearrangements. (K), heavy chain VDJ rearrangements. (L), kappa light chain VJ rearrangements.
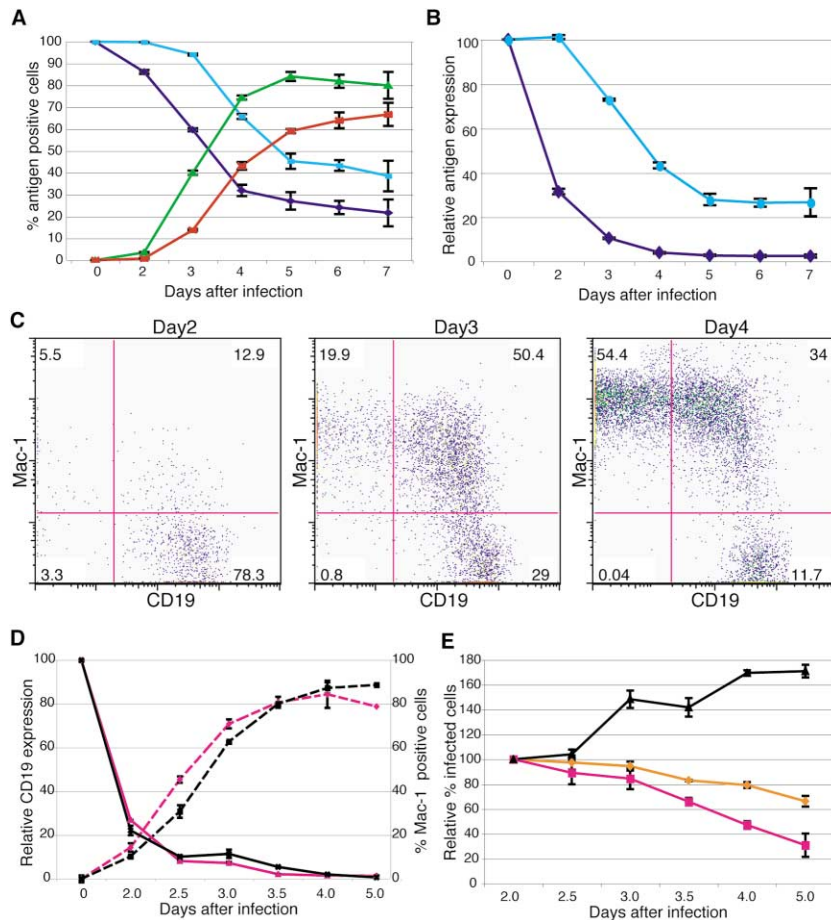
Figure 4. Reprogramming Kinetics of C/EBPα and β-Infected B Cell Precursors

(A) CD19⁺ precursors were infected with C/EBPα virus and percent antigen-positive cells scored at different times. CD19, dark blue; B220, light blue; Mac-1, green; Gr-1, red.

(B) Same as in (A), except that fluorescent intensities of infected versus uninfected cells (100%) were plotted.

(C) CD19⁺ bone marrow cells infected with C/EBPβ virus and cultured for 2–4 days.

(D) Comparison of C/EBPα- and C/EBPβ-induced CD19 downregulation and Mac-1 upregulation. Pink lines, cells infected with C/EBPα virus; black lines, cells infected with C/EBPβ. Solid lines, CD19; broken lines, Mac-1. Similar differences in the kinetics were observed in another experiment.

(E) Percentage of infected cells recovered over time, relative to the percentage of infected cells at day 2. Black line, C/EBPβ virus; orange line, control virus; pink line, C/EBPα virus-infected cells. All experiments were done in triplicate wells, with values showing the means and standard deviations.

C/EBPβ versus C/EBPα

Our data show that C/EBPβ is capable of reprogramming B cells at similar efficiencies as C/EBPα (∼60% of infected B cell precursors). However, the two proteins differ in that enforced expression of C/EBPα leads to cell loss, while C/EBPβ-overexpressing cells are induced to proliferate. This suggests that the rate of cell division is irrelevant for the reprogramming process and that the percentages of induced macrophages observed reflect the actual reprogramming frequency. The growth-arresting potential of C/EBPα and the proliferation-inducing potential of C/EBPβ have been described before for a number of cell systems. For example, during hormonally induced adipocyte differentiation of preadipocytes, C/EBPβ induces mitotic clonal expansion, followed by the activation of C/EBPα, terminal differentiation, and growth arrest (Tang et al., 2003). Whether C/EBPβ also activates C/EBPα expression in our system remains to

be determined. Another important question that needs to be addressed is why the apparent upregulation of full-length C/EBPβ during normal B cell development (Cooper et al., 1994) does not lead to their reprogramming into macrophages.

Parallel and Sequential Reprogramming Mechanisms Induced by C/EBP

Our data indicate that C/EBP acts by a two-pronged approach (Figure 7B) by downregulating the late B cell-specific marker CD19 through inhibition of Pax5 on the one hand and by upregulating myeloid genes on the other. The observed synergism between C/EBP with PU.1 is in line with the fact that most myeloid promoters require both C/EBP and PU.1 for efficient activation (Friedman, 2002; Tenen et al., 1997). Likewise, our studies support reports that C/EBPα can activate PU.1 expression and that PU.1 can positively regulate its own
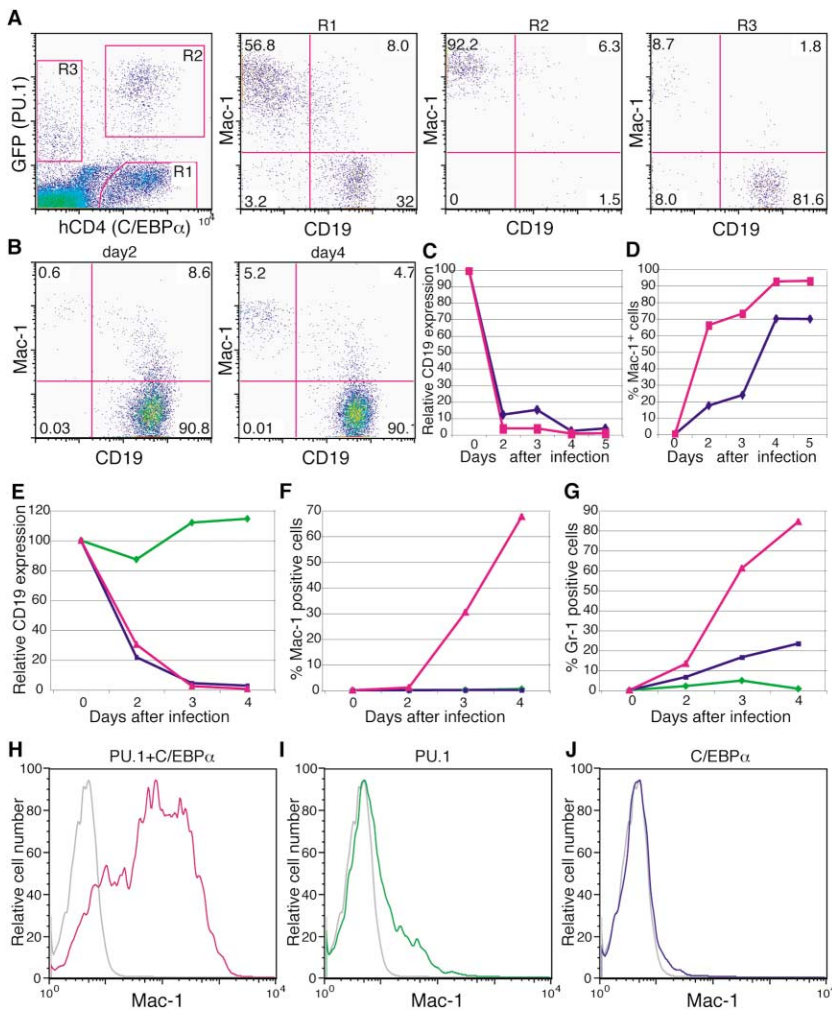
Figure 5. Role of PU.1 in C/EBPα-Induced Reprogramming

(A–D) Effects of double infection with C/EBPα and PU.1 viruses on B cell reprogramming efficiency and Mac-1 upregulation. (A) CD19+ bone marrow precursors were coinfected with PU.1-GFP and C/EBPα-hCD4 virus and analyzed 4 days later. Profile on the left shows C/EBPα virus-only-infected cells (R1), double-infected cells (R2), and PU.1 virus-infected cells (R3). The corresponding phenotypes are shown in the three profiles to the right. (B) CD19+ cells singly infected with PU.1 virus 2 and 4 days after infection. (C) Kinetics of CD19 and (D), Mac-1 antigen expression of cells shown in (A). Red curves, double-infected cells; blue curves, C/EBPα virus-only-infected cells. CD19 values correspond to relative mean fluorescent intensity and Mac-1 values to percent CD19−Mac-1+ infected cells.

(E–J) PU.1-independent and PU.1-dependent changes induced by C/EBPα. (E–G) PU.1−/− pre-B cells were coinfected with C/EBPα-hCD4 and PU.1-GFP virus, and singly and doubly infected cells were gated at various times thereafter and analyzed for expression of CD19 (E), Mac-1 (F), and Gr-1 (G). Red lines, double-infected cells; green lines, PU.1-infected cells; blue lines, C/EBPα-infected cells. (H–J) NIH3T3 fibroblasts were coinfected with C/EBPα-hCD4 and PU.1-GFP virus and analyzed for Mac-1 antigen expression 4 days later. The data show overlayed histograms of uninfected control cells (gray lines) with the infected cells, colorcoded as in (E)–(G).

(high-level) expression in macrophages (reviewed in Friedman [2002]). The antagonism of C/EBP toward Pax5 has not been described before. It will be interesting to determine its mechanism.

Several observations suggest that at least one additional reprogramming event is required for the completion of the C/EBP-induced B to M conversion. First, there is a 2 day delay in the downregulation of the early B cell antigen B220 compared to CD19 (Figure 4B). Since B220 is an alternatively spliced form of CD45, a panhematopoietic marker which we found to be expressed in reprogrammed macrophages, this is likely to reflect the inactivation of a B lineage-specific component of the splicing machinery. Second, reprogrammed macrophages

not only exhibit an extinction of the Pax5-regulated CD19 gene but also that of the early regulators EBF and E2A as well as of a number of their downstream targets, including Pax5. Their extinction, on the other hand, cannot be explained by the inactivation of Pax5 alone, since the protein is neither known to regulate its own expression nor to activate E2A or EBF. In addition, Pax5−/− pro-B cells express B220 and maintain their lymphoid identity when maintained in the presence of IL-7, although a number of myeloid genes are derepressed (Nutt et al., 1999). We therefore postulate that an additional, early B cell regulator becomes inactivated during the reprogramming process. This might happen through yet another direct action of C/EBP or indirectly, such
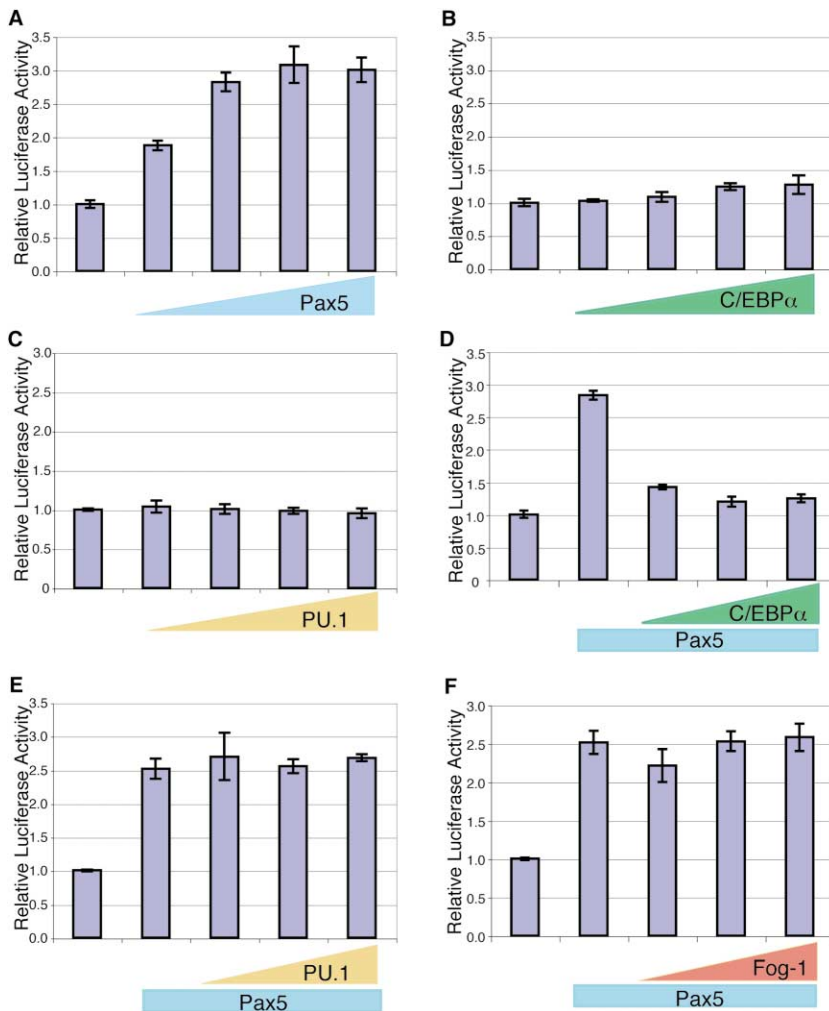
Figure 6. Effects of C/EBPα and PU.1 on the Pax5-Mediated Activation of the CD19 Promoter

293 cells were cotransfected with a reporter plasmid consisting of a 1.3 kb upstream fragment of the human CD19 promoter linked to the firefly luciferase gene, together with transcription factor-encoding retroviral vectors and a β-gal control plasmid. (A–C) Effect of increasing concentrations of Pax5, C/EBPα, and PU.1 DNA on the CD19 promoter. (C–F) Effects of increasing concentrations of C/EBPα, PU.1, and FOG-1 DNA on suppression of the ability of Pax5 to drive the expression of the CD19 promoter. Values shown, corrected for transfection efficiency, correspond to means ±SD obtained from three separate wells.

as through PU.1 expressed at elevated levels (Figure 7B). We favor the latter possibility, because enforced expression of PU.1 on its own can reprogram a proportion of early B cell precursors, showing a delayed downregulation of CD19 expression compared to C/EBP-infected cells and because it is unable to inactivate Pax5 on the CD19 promoter. Experiments with inducible versions of C/EBP should offer further insights into the sequential extinction of the B cell gene expression program and whether B cells become irreversibly committed to a myeloid fate after a limited exposure to exogenous C/EBP. Similar experiments with chicken MEP cells have revealed that a 2–3 day activation of exogenous C/EBPβ or PU.1 is sufficient to induce their commitment into either eosinophils or myeloid cells, respectively (Nerlov and Graf, 1998; Nerlov et al., 1998).

Role of Dosage
Our results indicate that the B to M conversion frequency depends on the dosage of C/EBP. In addition, the dos-

age of endogenous PU.1 also matters. The fact that C/EBP-induced upregulation of myeloid genes strictly requires PU.1 and that C/EBP nonresponders can be reprogrammed through coinfection with PU.1 (Figure 5A) suggests that the latter express subthreshold levels of endogenous PU.1. In addition, initially, some responders predominantly downregulate CD19, while others predominantly upregulate Mac-1 (Figure 1D). This could be explained by the assumption that the former express relatively low levels of endogenous PU.1 before infection, resembling PU.1$^{-/-}$ cells in their response to C/EBPα (Figures 5E–5G), while the latter represent cells with relatively high levels of PU.1, resembling C/EBPα/PU.1 double-infected cells (Figure 5A) in their response. However, we cannot rule out the possibility that the observed heterogeneity in the C/EBP response reflects differences between individual cells in CD19 degradation and Mac-1 synthesis rates.

A role of transcription factor dosage for lineage determination has been suggested earlier, such as for GATA-1
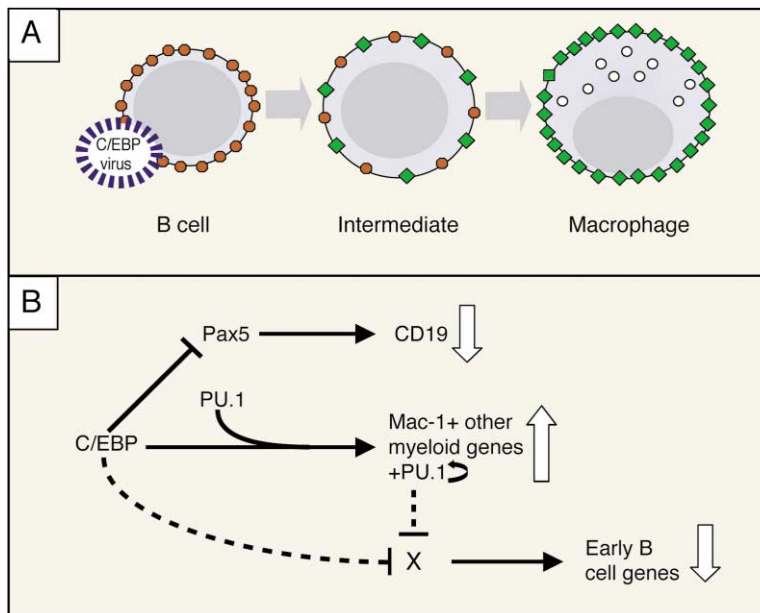
Figure 7. Summary of the Observed B Cell to Macrophage Conversion

(A) Changes occurring at the cell surface after infection of a CD19-expressing B cell with a C/EBP virus. The cell is shown to turn into Mac-1+ after passing through an intermediate that expresses low levels of CD19 and Mac-1 antigen. CD19, red circles; Mac-1, green squares.

(B) Changes occurring inside the nucleus. Straight arrows and T-shaped bars indicate activation and inhibition, respectively. Curved arrow, autoregulation; open arrows, up- or downregulation. Dashed lines indicate uncertainty.

levels determining the decision between eosinophil and MEP cell formation (Kulessa et al., 1995) and of PU.1 levels for B cell and macrophage formation (DeKoter and Singh, 2000). The balance between the dosages of PU.1 and C/EBPα has also been shown to be important for the formation of macrophages versus granulocytes in vivo (Dahl et al., 2003). It was recently reported that C/EBPα can reprogram pro-B cells derived from Pax5$^{-/-}$ but not from wild-type mice (Heavey et al., 2003). This discrepancy might either be due to differences in culture conditions or to C/EBP expression levels achieved. We favor the latter explanation, since, in our study, only B cells with high levels of ectopic C/EBPα expression became efficiently reprogrammed. The present work, together with experiments showing that the expression of myeloid genes (such a *M-CSFR*) is activated when Pax5 is ablated in pro-B cells (Mikkola et al., 2002), indicates that C/EBP and Pax5 act in a cross-antagonistic manner. In support of this is the observation that coinfection of B cell precursors with C/EBPα and Pax5 leads to a reduced reprogramming frequency compared to C/EBPα alone (our unpublished data). Similarly, work with hematopoietic cell lines has shown that the balance of GATA-1 and PU.1 and of FOG-1 and C/EBP determines whether cells become committed to either the erythroid or myelomonocytic lineages (Cantor and Orkin, 2001; Graf, 2002), with cells capable of differentiating in both directions.

Induced Remodeling of a Transcription Factor Network: A Model for Normal Differentiation?
Hematopoietic lineages are established and maintained by cell type-specific regulatory circuits or transcription factor "networks" (Sieweke and Graf, 1998; Warren and Rothenberg, 2003). Thus, during B cell commitment, the combination of E2A with EBF drives Pax5 expression, and all three factors regulate the expression of genes in differentiated cells (for review, see Hardy [2003] and Schebesta et al. [2002]). Likewise, C/EBPα and/or β to-

gether with PU.1^{high} drive the expression of macrophage-specific genes and also regulate each other as well as themselves, thus maintaining high levels of expression (Friedman, 2002; Nerlov and Graf, 1998; Tenen et al., 1997). From this perspective, our data suggest that enforced expression of C/EBP in B cells alters the configuration of the B cell transcription factor network by simultaneously modulating the activity and level of two of its components (Pax5 and PU.1). We speculate that, under the influence of high PU.1 levels, this intermediate network configuration is not stable, resulting in the formation of a macrophage-specific transcription factor network. The new configuration is then stabilized by auto- and crossregulation of PU.1 and C/EBP gene expression. Our data suggest that the choice of a fetal liver precursor to become either a B cell or a macrophage might obey similar rules. It is possible that, in these progenitors, both C/EBP and Pax5 are expressed at low levels and that during differentiation, one factor becomes dominant through the mechanism described.

Does the B Cell to Macrophage Conversion Recapitulate a Pathological Process?
The speed and efficiency with which B cell precursors can be reprogrammed by C/EBPα (and C/EBPβ) raise the question as to whether this process can be induced under pathological conditions. Thus, infection of B cells with specific pathogens, or other stresses that activate signaling pathways, might activate C/EBPα or C/EBPβ and convert them into macrophages. In this context, it is interesting that reprogramming of pro-T1 cells into myeloid cells by ectopic GM-CSFR signaling is accompanied by C/EBPα expression (Iwasaki-Arai et al., 2003). Our finding that even relatively mature B cells retain considerable plasticity may also be relevant for the pathogenesis of leukemia. Thus, some myeloid leukemias exhibit immunoglobulin gene rearrangements (Mirro et al., 1986). Also, Hodgkin's lymphoma cells, which express some genes shared with monocytic and

dendritic cells but lack most B cell markers, typically contain immunoglobulin rearrangements and somatic hypermutations (Kuppers et al., 2002), suggesting a germinal center B cell origin.

Experimental Procedures

Mouse Strains and Purification of B Lineage Cells
CD19 Cre-ROSA EYFP mice (+/Ki, +/Ki) have been described previously (Ye et al., 2003). RAG2$^{-/-}$γc$^{-/-}$ mice were purchased from Taconic. To obtain B cell precursors, bone marrow cells from 5-week-old mice were harvested from hindleg bones. After lysis of erythroid cells, they were suspended in PBS with 4% FCS and incubated with Fc-block (BD Pharmingen) for 10 min followed by 20 min incubation on ice with biotinylated anti-mouse CD19 or B220 antibodies (BD Pharmingen). Cells were washed with PBS/2 mM EDTA twice and then resuspended at 10^7 cells/90 μl. To this, 10 μl of streptavidin-coated microbeads were added and incubated on ice for 20 min. After two washes with PBS/FCS, cells were pelleted and resuspended at 10^8 cells/500 μl. Cell separations were carried out with Auto-MACS (Miltenyi Biotech) using the POSSELD program. Sorted cells were stained with PE-CD19, APC-Mac-1 antibodies (BD Pharmingen), and analyzed by flow cytometry on a FACSCalibur (BD Biosciences).

Transcription Factor-Encoding Vectors
Retroviruses encoding full-length cDNAs of murine PU.1, C/EBPα, and Pax5 (Nerlov and Graf, 1998; Nerlov et al., 1998) were cloned by PCR into the BglII/XhoI sites of the pMIG retrovirus vector by creating a BglII site on the 5′ end and a XhoI site at the 3′ end, while full-length murine C/EBPβ (gift from Dr. Philip Scherer) was inserted into the EcoRI site of the vector. The hCD4 virus vector was generated by removing the GFP sequence from pMIG with NcoI/SalI and inserting a truncated hCD4 excised from pMACS4.1 (Sigma) by NotI/HindIII using blunt end ligation. MMP-HA-FOG was a gift from Dr. Stuart Orkin.

Retrovirus Production, Infection, Cell Culture, and Transplantation
Retrovirus stocks were prepared by transient transfection of Phoenix-Eco cells (gift from Dr. Garry Nolan) using Lipofectamine Plus (Life Technologies), and supernatants were harvested 48 hr later. For infection, purified B cells were resuspended at 5 × 10^5 cells/ml in RPMI1640 with 10% FCS, 5.5 × 10^{-5}M 2-mercaptoethanol as well as 10 ng/ml each of IL-3, IL-7, Flt-3, SCF, and M-CSF (R&D Systems). Then, 2 ml aliquots were deposited into a 12-well plate precoated with retronectin (Takara) followed by 2 ml of retrovirus supernatant to which polybrene (Sigma) was added (8 μg/ml). The plates were centrifuged for 60 min at 700 × g, followed by 3–6 hr of incubation at 32°C. Infected cells were then transferred onto irradiated (3000 rad) S17 stromal cells supplemented with 10 ng/ml of IL-3, IL-7, Flt-3, SCF, and M-CSF or transplanted intravenously (4 × 10^6 cells/mouse) into sublethally irradiated (280 rad) RAG2$^{-/-}$γc$^{-/-}$ mice.

FACS Analysis and Phagocytosis Assay
Biotinylated antibodies against CD19, B220, Mac-1; PE-labeled CD19, B220, Mac-1, Gr-1; and APC-labeled B220, Mac-1, Gr-1, and L-selectin antibodies were purchased from BD Pharmingen; PE-Cy7-hCD4, APC-F4/80 from Caltag; and PE-conjugated anti-IgM, -IgD, -IgG, -Ig kappa, and -Ig lambda from Southern Biotechnology Associates, Inc. Stained cell samples were run on FACScalibur and LSRII (BD Biosciences) machines and data analyzed with FlowJo software (Tree Star). For phagocytosis assays, S17 stromal cells and B cells were removed from C/EBPα-infected cultures (18 days postinfection) by vigorous pipetting. The remaining adherent cells were incubated with 0.5 μl of 1 μm red fluorescent carboxylated microspheres (Molecular Probes) for 1 hr at 37°C in RPMI 1640 plus 10% FCS and 10 ng/ml M-CSF. The cells were then thoroughly washed, stained with Hoechst 33342, and photographed using EnDow GFP, TRITC, and cyan GFP filters. Images were superimposed on a bright field image using Metamorph software (Universal Imaging Corporation).

FACS Sorting and Semiquantitative RT-PCR
Reprogrammed cells derived from CD19 ancestry mice (EYFP$^+$hCD-4$^+$CD19$^-$Mac-1$^+$) cultured for 10 days were sorted in a MoFlo cell sorter (Cytomation). Control populations were also sorted. Total RNA was extracted from each population as well as from MACS-purified CD19 or Mac-1$^+$ cells using Trizol (Life Technologies). RNA was digested with RNase-free DNase I (Roche) to remove contaminating genomic DNA. Then first-strand cDNA was synthesized with SuperScript II RNase H reverse transcriptase using oligo (dT)$_{12-18}$ primer (Life Technologies). Concentration of cDNA in different samples was calibrated by β actin cDNA. PCR reactions were run at 94°C for 2 min (denaturation) followed by 94°C for 30 s, 60°C for 30 s, and 72°C for 30 s for 26–33 cycles (amplification), depending on the relative abundance of mRNA from different genes. PCR products were resolved on agarose gels and visualized by ethidium bromide staining. Images were taken by ChemiImager 4400 (Alpha Innotech Corporation) and quantitated with ImageQuant V1.2 software (Molecular Dynamics). For primers used, see Supplemental Table S3.

Immunoglobulin Gene Rearrangements
Reprogrammed cells from CD19 ancestry mice (cultured for 18 days) were sorted as above. As a control, adherent macrophages (CD19$^-$Mac-1$^+$) derived from bone marrow cultured under the same conditions were also sorted. Freshly isolated spleen cells were used as another control. Genomic DNA was extracted using DNeasy Tissue Kit (Qiagen). DNA from about 600 reprogrammed cells and 1600 control macrophages cells was used for PCR reactions. These were run at 94°C for 2 min (denaturation) followed by 94°C for 15 s, 60°C for 30 s, and 72°C for 60 s for 40 cycles (amplification). For D$_H$J$_H$ rearrangements, the primer pair D$_{FS}$ and J$_H$4A was used. For V$_H$D$_H$J$_H$ rearrangements, V$_H$A, V$_H$B, V$_H$C, V$_H$D, V$_H$E, and V$_H$F 5′ primers were used in separate reactions together with J$_H$4E as a 3′ primer (Ehlich et al., 1994). The primers for kappa light chain rearrangement V$_κ$, J$_κ$2, J$_κ$5 were as described (ten Boekel et al., 1995). PCR products were resolved on agarose gels and visualized by ethidium bromide staining. Images were taken by ChemiImager 4400 (Alpha Innotech Corporation). DNA bands corresponding to V$_H$AJ$_H$3, V$_H$EJ$_H$2, V$_H$EJ$_H$4, V$_H$FJ$_H$4, V$_κ$J$_κ$1, V$_κ$J$_κ$2, and V$_κ$J$_κ$5 were cloned and verified by sequencing.

Cell Lines
The S17 stromal cell line was a gift from Dr. Gordon Keller. The PU.1$^{-/-}$ cell line was derived from a conditional knockout mouse line (Drs. H. Iwasaki, D. Tenen, and K. Akashi, personal communication), in which exons 4 and 5 were removed by crossing it with a β actin Cre mouse. The particular cells used were derived from a 16 day fetal liver and had been maintained on irradiated S17 cells plus 10 μg/ml SCF, 10 μg/ml IL-3, and 5 μg/ml IL-7 for 5 months. Its lack of exons 4 and 5 was confirmed by PCR.

CD19 Promoter Reporter Assay
The CD19 promoter reporter (Kozmik et al., 1992) (gift from Dr. Meinrad Busslinger) contains a 1.3 kb fragment of the human CD19 promoter sequence linked to firefly luciferase cDNA and inserted into the plasmid pSP64. CD19-Luc reporter plasmid (0.3 μg) was used for transfection of 293 cells grown in 12-well plates. CMV-β-gal (0.05 μg) was used as an internal control. To test dosage effects, 0.01, 0.05, 0.1, and 0.3 μg of Pax5, C/EBPα, PU.1, and FOG-1 DNA in pMIG retrovirus vector were adjusted to a total of 0.3 μg DNA with control pMIG vector DNA. For inhibition experiments, 0.05 μg of Pax5 expression vector was transfected together with 0.05, 0.1, and 0.25 μg of C/EBPα, PU.1, and FOG-1 DNAs. After transfection (36–48 hr), cells were lysed with 250 μl of passive lysis buffer (Promega) and 20 μl of the lysate used to measure luciferase activity (luciferase substrate was from Promega Life Sciences) using AutoLumat Plus LB 953 luminometer (Berthold Technology). Another 20 μl was used to measure β-galactosidase activity to calibrate luciferase values. All samples were tested in triplicate.

References

Akashi, K., Reya, T., Dalma-Weiszhausz, D., and Weissman, I.L. (2000a). Lymphoid precursors. Curr. Opin. Immunol. *12*, 144–150.

Akashi, K., Traver, D., Miyamoto, T., and Weissman, I.L. (2000b). A clonogenic common myeloid progenitor that gives rise to all myeloid lineages. Nature *404*, 193–197.

Borzillo, G.V., Ashmun, R.A., and Sherr, C.J. (1990). Macrophage lineage switching of murine early pre-B lymphoid cells expressing transduced fms genes. Mol. Cell. Biol. *10*, 2703–2714.

Cantor, A.B., and Orkin, S.H. (2001). Hematopoietic development: a balancing act. Curr. Opin. Genet. Dev. *11*, 513–519.

Chen, X., Liu, W., Ambrosino, C., Ruocco, M.R., Poli, V., Romani, L., Quinto, I., Barbieri, S., Holmes, K.L., Venuta, S., and Scala, G. (1997). Impaired generation of bone marrow B lymphocytes in mice deficient in C/EBPbeta. Blood *90*, 156–164.

Chevillard, C., Ozaki, J., Herring, C.D., and Riblet, R. (2002). A three-megabase yeast artificial chromosome contig spanning the C57BL mouse Igh locus. J. Immunol. *168*, 5659–5666.

Cooper, C.L., Berrier, A.L., Roman, C., and Calame, K.L. (1994). Limited expression of C/EBP family proteins during B lymphocyte development. Negative regulator Ig/EBP predominates early and activator NF-IL-6 is induced later. J. Immunol. *153*, 5049–5058.

Dahl, R., Walsh, J.C., Lancki, D., Laslo, P., Iyer, S.R., Singh, H., and Simon, M.C. (2003). Regulation of macrophage and neutrophil cell fates by the PU.1:C/EBPalpha ratio and granulocyte colony-stimulating factor. Nat. Immunol. *4*, 1029–1036.

DeKoter, R.P., and Singh, H. (2000). Regulation of B lymphocyte and macrophage development by graded expression of PU.1. Science *288*, 1439–1441.

Ehlich, A., Martin, V., Muller, W., and Rajewsky, K. (1994). Analysis of the B-cell progenitor compartment at the level of single cells. Curr. Biol. *4*, 573–583.

Friedman, A.D. (2002). Transcriptional regulation of granulocyte and monocyte development. Oncogene *21*, 3377–3390.

Geissmann, F., Jung, S., and Littman, D.R. (2003). Blood monocytes consist of two principal subsets with distinct migratory properties. Immunity *19*, 71–82.

Graf, T. (2002). Differentiation plasticity of hematopoietic cells. Blood *99*, 3089–3101.

Hardy, R.R. (2003). B-cell commitment: deciding on the players. Curr. Opin. Immunol. *15*, 158–165.

Heavey, B., Charalambous, C., Cobaleda, C., and Busslinger, M. (2003). Myeloid lineage switch of Pax5 mutant but not wild-type B cell progenitors by C/EBPalpha and GATA factors. EMBO J. *22*, 3887–3897.

Heyworth, C., Pearson, S., May, G., and Enver, T. (2002). Transcription factor-mediated lineage switching reveals plasticity in primary committed progenitor cells. EMBO J. *21*, 3770–3781.

Hume, D.A., Ross, I.L., Himes, S.R., Sasmono, R.T., Wells, C.A., and Ravasi, T. (2002). The mononuclear phagocyte system revisited. J. Leukoc. Biol. *72*, 621–627.

Iwasaki, H., Mizuno, S., Wells, R.A., Cantor, A.B., Watanabe, S., and Akashi, K. (2003). GATA-1 converts lymphoid and myelomonocytic

progenitors into the megakaryocyte/erythrocyte lineages. Immunity *19*, 451–462.

Iwasaki-Arai, J., Iwasaki, H., Miyamoto, T., Watanabe, S., and Akashi, K. (2003). Enforced granulocyte/macrophage colony-stimulating factor signals do not support lymphopoiesis, but instruct lymphoid to myelomonocytic lineage conversion. J. Exp. Med. *197*, 1311–1322.

Jones, L.C., Lin, M.L., Chen, S.S., Krug, U., Hofmann, W.K., Lee, S., Lee, Y.H., and Koeffler, H.P. (2002). Expression of C/EBPbeta from the C/ebpalpha gene locus is sufficient for normal hematopoiesis in vivo. Blood *99*, 2032–2036.

Katsura, Y. (2002). Redefinition of lymphoid progenitors. Nat. Rev. Immunol. *2*, 127–132.

Kee, B.L., and Murre, C. (2001). Transcription factor regulation of B lineage commitment. Curr. Opin. Immunol. *13*, 180–185.

King, A.G., Kondo, M., Scherer, D.C., and Weissman, I.L. (2002). Lineage infidelity in myeloid cells with TCR gene rearrangement: a latent developmental potential of proT cells revealed by ectopic cytokine receptor signaling. Proc. Natl. Acad. Sci. USA *99*, 4508–4513.

Klinken, S.P., Alexander, W.S., and Adams, J.M. (1988). Hemopoietic lineage switch: v-raf oncogene converts Emu-myc transgenic B cells into macrophages. Cell *53*, 857–867.

Kondo, M., Scherer, D.C., Miyamoto, T., King, A.G., Akashi, K., Sugamura, K., and Weissman, I.L. (2000). Cell-fate conversion of lymphoid-committed progenitors by instructive actions of cytokines. Nature *407*, 383–386.

Kozmik, Z., Wang, S., Dorfler, P., Adams, B., and Busslinger, M. (1992). The promoter of the CD19 gene is a target for the B-cell-specific transcription factor BSAP. Mol. Cell. Biol. *12*, 2662–2672.

Kulessa, H., Frampton, J., and Graf, T. (1995). GATA-1 reprograms avian myelomonocytic cell lines into eosinophils, thromboblasts, and erythroblasts. Genes Dev. *9*, 1250–1262.

Kuppers, R., Schwering, I., Brauninger, A., Rajewsky, K., and Hansmann, M.L. (2002). Biology of Hodgkin's lymphoma. Ann. Oncol. *13*, 11–18.

Mikkola, I., Heavey, B., Horcher, M., and Busslinger, M. (2002). Reversion of B cell commitment upon loss of Pax5 expression. Science *297*, 110–113.

Mirro, J., Kitchingman, G.R., Williams, D.L., Murphy, S.B., Zipf, T.F., and Stass, S.A. (1986). Mixed lineage leukemia: the implications for hematopoietic differentiation. Blood *68*, 597–599.

Nerlov, C., and Graf, T. (1998). PU.1 induces myeloid lineage commitment in multipotent hematopoietic progenitors. Genes Dev. *12*, 2403–2412.

Nerlov, C., McNagny, K.M., Doderlein, G., Kowenz-Leutz, E., and Graf, T. (1998). Distinct C/EBP functions are required for eosinophil lineage commitment and maturation. Genes Dev. *12*, 2413–2423.

Nutt, S.L., Heavey, B., Rolink, A.G., and Busslinger, M. (1999). Commitment to the B-lymphoid lineage depends on the transcription factor Pax5. Nature *401*, 556–562.

Orkin, S.H. (2000). Diversification of haematopoietic stem cells to specific lineages. Nat. Rev. Genet. *1*, 57–64.

Pahl, H.L., Scheibe, R.J., Zhang, D.E., Chen, H.M., Galson, D.L., Maki, R.A., and Tenen, D.G. (1993). The proto-oncogene PU.1 regulates expression of the myeloid-specific CD11b promoter. J. Biol. Chem. *268*, 5014–5020.

Poli, V. (1998). The role of C/EBP isoforms in the control of inflammatory and native immunity functions. J. Biol. Chem. *273*, 29279–29282.

Radomska, H.S., Huettner, C.S., Zhang, P., Cheng, T., Scadden, D.T., and Tenen, D.G. (1998). CCAAT/enhancer binding protein alpha is a regulatory switch sufficient for induction of granulocytic development from bipotential myeloid progenitors. Mol. Cell. Biol. *18*, 4301–4314.

Schebesta, M., Heavey, B., and Busslinger, M. (2002). Transcriptional control of B-cell development. Curr. Opin. Immunol. *14*, 216–223.

Screpanti, I., Romani, L., Musiani, P., Modesti, A., Fattori, E., Lazzaro, D., Sellitto, C., Scarpa, S., Bellavia, D., Lattanzio, G., et al.

(1995). Lymphoproliferative disorder and imbalanced T-helper response in C/EBP beta-deficient mice. EMBO J. *14*, 1932–1941.

Sieweke, M.H., and Graf, T. (1998). A transcription factor party during blood cell differentiation. Curr. Opin. Genet. Dev. *8*, 545–551.

Tang, Q.Q., Otto, T.C., and Lane, M.D. (2003). CCAAT/enhancer-binding protein beta is required for mitotic clonal expansion during adipogenesis. Proc. Natl. Acad. Sci. USA *100*, 850–855.

ten Boekel, E., Melchers, F., and Rolink, A. (1995). The status of Ig loci rearrangements in single cells from different stages of B cell development. Int. Immunol. *7*, 1013–1019.

Tenen, D.G., Hromas, R., Licht, J.D., and Zhang, D.E. (1997). Transcription factors, normal myeloid development, and leukemia. Blood *90*, 489–519.

Warren, L.A., and Rothenberg, E.V. (2003). Regulatory coding of lymphoid lineage choice by hematopoietic transcription factors. Curr. Opin. Immunol. *15*, 166–175.

Ye, M., Iwasaki, H., Laiosa, C.V., Stadtfeld, M., Xie, H., Heck, S., Clausen, B., Akashi, K., and Graf, T. (2003). Hematopoietic stem cells expressing the myeloid lysozyme gene retain long-term, multilineage repopulation potential. Immunity *19*, 689–699.

Zhang, D.E., Zhang, P., Wang, N.D., Hetherington, C.J., Darlington, G.J., and Tenen, D.G. (1997). Absence of granulocyte colony-stimulating factor signaling and neutrophil development in CCAAT enhancer binding protein alpha-deficient mice. Proc. Natl. Acad. Sci. USA *94*, 569–574.